Nonlinear wave effects on dynamic responses of a semisubmersible floating offshore wind turbine in the intermediate water

IOP Conf. Series: Journal of Physics: Conf. Series **1037** (2018) 022037 doi:10.1088/1742-6596/1037/2/022037

Nonlinear wave effects on dynamic responses of a semisubmersible floating offshore wind turbine in the intermediate water

Jia Pan[1], Takeshi Ishihara[1]

[1]Department of Civil Engineering, School of Engineering, The University of Tokyo, Japan, 7-3-1 Hongo, Bunkyo, 113-8656

E-mail: pan@bridge.t.u-tokyo.ac.jp

Abstract. The effects of nonlinear wave on the dynamic responses of Floating Offshore Wind Turbines (FOWTs) in the intermediate water are investigated. Firstly, the predicted dynamic responses of FOWT by the stream function in various wave conditions are investigated and validated by the water tank tests. The effects of nonlinear wave on dynamic responses of FOWT are then examined by comparing response amplitude operators (RAO) and time histories of wave elevation, dynamic responses and mooring tensions predicted by linear and nonlinear wave theories. Finally, the power spectrum densities (PSD) of dynamic responses of FOWT are analysed to explain the nonlinear wave effects in the frequency domain.

1. Introduction

Floating Offshore Wind Turbine is a promising innovation. Some researches show that FOWTs are cost effective and are expected to produce more energy comparing with the fixed foundation at the water depth greater than 50m [1]. Some FOWTs are built and planed in the intermediate water, where the water depth is ranged between the deep and shallow waters. In WindFloat project, a 2MW FOWT with a semisubmersible foundation was installed in 2011 at 5km offshore of Portugal, where the water depth is about 40m and the waves exceed 17 meters in height [2]. In Japan, NEDO plans to construct a 3MW FOWT with a pontoon foundation at City of Kitakyushu in a site with about 50m water depth.

The wave theory is important for the design of offshore wind turbines and the nonlinearity of waves are considered for the fixed offshore wind turbines in the shallow water. Aharwal and Manuel (2011) [3] and Van Der Meulen et al. (2012) [4] applied the second order wave theory to predict the extreme and fatigue loads for the fixed foundations and compared with those by the traditional linear wave theory. Ishihara and Phuc (2007) [5] investigated the effect of nonlinear wave on the dynamic responses of a floating offshore wind turbine system and showed the dynamic responses of bending moment at 50m water depth is 1.8 times larger than these at 200m water depth. It indicated that the nonlinear waves may cause larger extreme loads in the intermediate water. However, the systematic studies of dynamic responses of FOWTs in the intermediate water are limited.

The several wave theories have been proposed and used in offshore engineering [6][7]. Airy wave theory is a common approach to produce the linear regular waves. The stream function to generate the nonlinear regular waves was first developed by Dean (1965) [8] and the numerical solution was obtained from the governing equation of velocity potential to satisfy the Laplace equation and nonlinear boundary conditions.

In this study, the applicability of linear and nonlinear wave theories are investigated to predict the dynamic responses of a semisubmersible FOWT in the intermediate water. Firstly, numerical models for prediction of dynamic responses and a water tank test are presented in section 2. The predicted dynamic responses by the nonlinear wave theory are then validated by the water tank test and are discussed in the linear, weak nonlinear and strong nonlinear regions in section 3. The conclusions obtained from this study are summarised in section 4.

2. Numerical models and water tank tests

Hydrodynamic models and wave theories used in this study are described in the section. The dynamic responses of 1/50 scaled FOWT employed in Fukushima FOREARD project [9] is investigated under various sea states conditions in water depths of 1.0m and used to validate the numerical models .

2.1. Hydrodynamic models

The equation of motion for the coupled simulating tower and support platform system can be written as follows:

$$\left(M_{ij}+A_{ij}\right)\ddot{q}_j+C_{ij}\dot{q}_j+K_{ij}q_j=F_{Gi}+F_{Bi}+F_{Hi}+F_{Mi}+F_{Ri} \tag{1}$$

where M_{ij}, C_{ij} and K_{ij} are the mass matrix, damping matrix and stiffness matrix respectively, A_{ij} is the full added mass matrix, q_j, $\dot{q}_j$, $\ddot{q}_j$ are the unknown displacements relative to the earth at the specified reference origin and their time derivatives, F_{Gi} is the gravitational force, F_{Bi} is the buoyancy force, F_{Hi} is the hydrodynamic force, F_{Mi} is the mooring tension, F_{Ri} is the restoring force, and the wind load is ignored in this study. The subscripts i and j express the degrees of freedom of the model and 6 degrees of freedom are considered..

The hydrodynamic forces contain Froude-Krylov force, diffraction force and viscous drag force as follows:

$$F_{Hi}=\left(1+C_{ai}\right)\rho V\dot{\boldsymbol{u}}_i+\sum 1/2\rho C_{dik}A_k(\boldsymbol{u}_i-\dot{\boldsymbol{q}}_i)|(\boldsymbol{u}_i-\dot{\boldsymbol{q}}_i)| \tag{2}$$

where V is the volume displaced by the model, the added mass coefficient C_a is specified by a full matrix obtained by the potential theory and acting on the reference centre of model. The drag coefficients C_{dik} are assumed acting on the component k of model in the i degree of freedom in Table1 according to the references[10][11]. u, $\dot{u}$ are the local water particle velocity and acceleration relative to the earth obtained by the wave kinematics models and will be describe in the section 2.2.

Table 1. Hydrodynamic parameters for each component of the platform.

	SF1	SF2/3	CF	Pn1	Pn2/3	CC	SC1	SC2/3	Br1	Br2/3	Moor
C_{a11}	0.3	0.4	0.3	0.01	1.0	1.1	1.0	1.1	0.4	1.4	1.0
C_{a33}	1.6	1.6	1.9	1.6	1.6	0	0	0	0.4	0.4	0.5
C_{d11}	0.9	1.5	1.1	0.07	2.1	0.9	0.6	1.3	0.2	1.3	2.6
C_{d33}	4.8	4.8	4.4	0	0	0	0	0	0	0	1.2

The integrated form for C_a is derived as Eq. (3) and compared with that by the potential theory as shown in Eq. (4):

$$\begin{aligned} C_{a11}&=\frac{1}{\rho V}\sum_{i=1}^{N}C_{a11}^{i}\rho V_i, \qquad C_{a33}=\frac{1}{\rho V}\sum_{i=1}^{N}C_{a33}^{i}\rho V_i \\ C_{a55}&=\frac{1}{\rho VR^2}\left(\sum_{i=1}^{N}C_{a11}^{i}\rho V_i z_i^2+\sum_{i=1}^{N}C_{a33}^{i}\rho V_i x_i^2+\sum_{i=1}^{N}C_{a55}^{i}\rho V_i R_i^2\right) \end{aligned} \tag{3}$$

$$C_a^{aqwa}=\begin{bmatrix} 0.71 & 0.0 & 0.0 & 0.0 & -0.13 & 0.0 \\ 0.0 & 0.71 & 0.0 & 0.13 & 0.0 & 0.0 \\ 0.0 & 0.0 & 0.99 & 0.0 & 0.0 & 0.0 \\ 0.0 & 0.13 & 0.0 & 0.09 & 0.0 & 0.0 \\ -0.13 & 0.0 & 0.0 & 0.0 & 0.09 & 0.0 \\ 0.0 & 0.0 & 0.0 & 0.0 & 0.0 & 0.09 \end{bmatrix} \quad C_a^{\text{integrated}}=\begin{bmatrix} 0.72 & 0.0 & 0.0 & 0.0 & -0.13 & 0.0 \\ 0.0 & 0.72 & 0.0 & 0.01 & 0.0 & 0.0 \\ 0.0 & 0.0 & 0.99 & 0.0 & 0.0 & 0.0 \\ 0.0 & 0.01 & 0.0 & 0.092 & 0.0 & 0.0 \\ -0.13 & 0.0 & 0.0 & 0.0 & 0.092 & 0.0 \\ 0.0 & 0.0 & 0.0 & 0.0 & 0.0 & 0.092 \end{bmatrix} \tag{4}$$

The difference between the potential theory and the integrated force model is negligible if the elements in the distributed force model are small enough, and the detail was shown in the reference [12]. C_d can be obtained by the same integrated form. The amplitude dependency of hydrodynamic coefficients is neglected since the effect of the nonlinear waves on dynamic responses is the main topic in this study. The software Orcaflex[13] is used for prediction of dynamic responses.

2.2. Wave theories

Two typical regular wave models representing linear and fully nonlinear waves are used in this study. Airy wave theory is the simplest wave theory for simulating linear regular wave, and the stream function represents a fully nonlinear regular wave. The elevation of linear regular wave surface can be shown as follows:

$$\eta_{LR}(t) = \frac{H}{2}\cos(kx - \omega t) \tag{5}$$

where H is the wave height, k is the wave number, and ω is the frequency of wave. In the linear wave, the wave crest height is the same as the wave through depth. And linear wave kinematics is used. The elevation of nonlinear regular wave surface generated by stream function can be expressed as :

$$\eta_{NR}(t) = \sum_{n=1}^{N} \alpha_n \cos\frac{2\pi n}{L}(x - ct) \tag{6}$$

where N is the order of stream function determined by the wave parameters and water depth, α_n is the unknown coefficients that can be calculated according to the boundary conditions, c is the propagation velocity of wave with respect to the water. Stream function can simulate waves from the linear wave (with $N = 1$) to the wave close to breaking wave height (with $N > 11$).

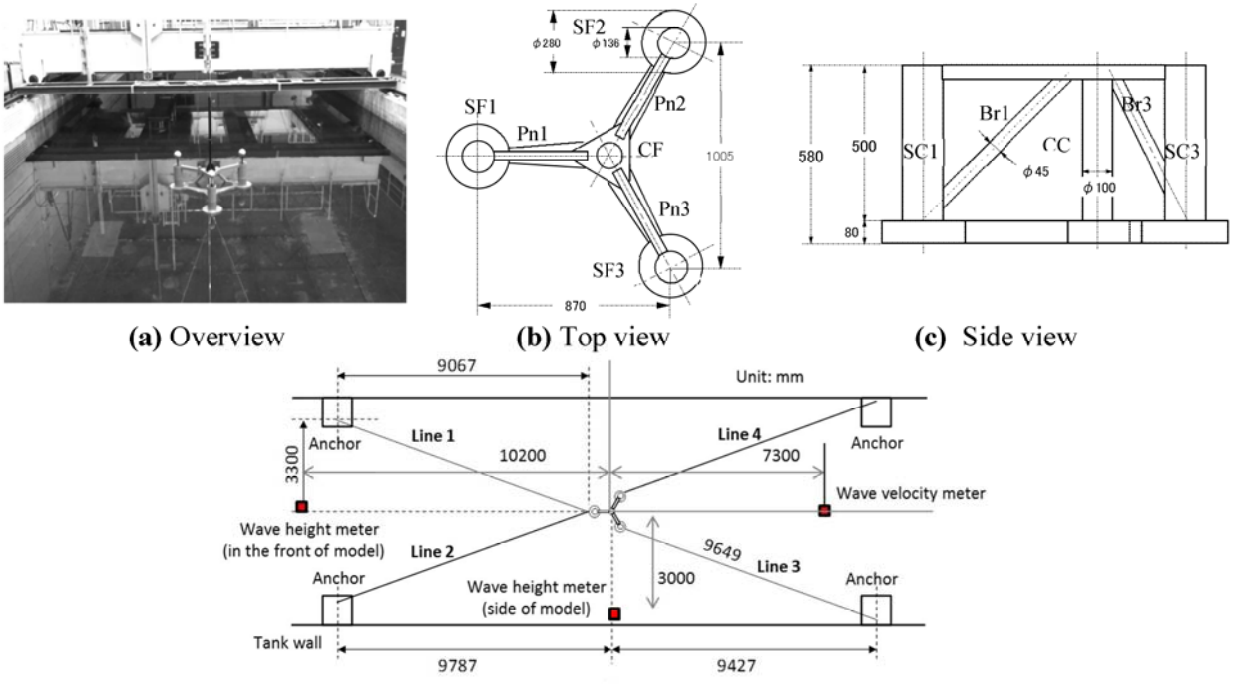

(a) Overview **(b)** Top view **(c)** Side view

(d) Configuration

Figure 1. Configuration and dimension of the model used in the water tank test.

2.3. Water tank test

A 1/50 scaled FOWT employed in Fukushima FOREARD project is used in the water tank test as shown in Figure 2. The tower and nacelle is simulated by a pole with a weight of 1.42kg and set on the

platform, while the detail of rotor is not considered in this model since the wind loads are not included in the water tank test. The total weight of the platform is 42.2kg and the model draft is 0.38m. In this semi-submersible FOWT, four mooring lines are connected with the three heave plates. The length of mooring line is 9.86m and the water depth is 1.0m. The fairlead is set on the heave plate and is located at 0.34m under the water surface. The wave height is measured at the front of model in the water tank test. The detail dimension of FOWT is shown in the top and side view of model in Fig. 1 (b) and (c). The mooring lines 1 and 2 are located in the upstream and the mooring lines 3 and 4 are in the downstream.

The static equilibrium test in still water is conducted to confirm the initial position of the platform and the initial fairlead tension in the mooring lines. Free decay tests in surge, sway, heave, roll, pitch and yaw directions in the still water are carried out to find the natural periods of platform in each degree of freedom (DOF). Time histories of platform motions in regular waves are measured. Unidirectional waves are used in the experiment.

2.4. Cases in water tank test and simulations

The cases of the water tank tests and simulations and various wave theories [7] are shown in Figure 2. In this study, three regions, namely, linear, week nonlinear and strong nonlinear regions are defined and dynamic responses of FOWT are considered in these regions. In the linear region, Airy wave theories and 1st order stream function are generally used. In the weak nonlinear region, Stokes's 5th and 3rd order stream function are selected in the diagram, where the nonlinearity of waves is not so strong. The strong nonlinear region is defined near the breaking waves. As the limitation of water tank test, it is difficult to generate very large wave, even FOWTs may endure such wave height in the real ocean environment. In this study, strong nonlinear waves are considered only in the simulations.

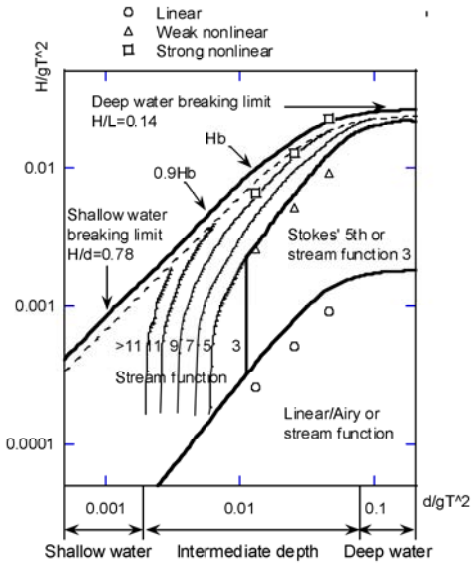

(a) Regular wave theory selection diagram in different water depths and wave conditions

	Height (m)	Period (s)	Ursell number
Linear region	0.02	1.5,	0.2
		2.0	0.5
		2.8	1.3
Weak nonlinear region	0.20	1.5	2.2
		2.0	5.4
		2.8	12.9
Strong nonlinear region	0.50	1.5	5.5
		2.0	13.5
		2.8	36.1

(b) Typical regular wave conditions in the water tank tests and simulations.

Figure 2. Typical regular wave conditions and that in regular wave theory selection diagram.

The Ursell number [14], which relates with the wave steepness parameter and shallow water parameter representing the nonlinearity of regular waves, is used to identify the nonlinearity of waves and is defined as follows:

$$U_R = S / \mu^3 = HL^2 / d^3 \tag{7}$$

where S is the wave steepness parameter and μ is the shallow water parameter, and H, L and d are the wave height, wave length and water depth respectively. It is clear that Ursell number increases

if the wave height and the wave length increase and the water depth becomes shallower. Some strong nonlinear waves cannot be generated in experiment due to the limitation of the water tank test in water depth of 1.0m.

Response amplitude operators (RAO) in the regular waves are used in this study. Fast Fourier Transform is employed to transform the time series to the amplitude of response in the frequency domain, and the dimensionless amplitude normalized by the half of wave height is shown as:

$$RAO_x = A_x / (H/2), RAO_z = A_z / (H/2), RAO_{\theta_y} = A_{\theta_y} / (H/2), RAO_{T_i} = A_{T_i} / p_0 BS \quad (8)$$

where A_x, A_z and A_{θ_y} are the amplitudes corresponding to the wave frequency component in surge, heave and pitch directions, and H refers to the wave height, A_{T_i} refers to the amplitude of fairlead tension in each mooring line, p_0 is the dynamic pressure at the water surface and is estimated as $p_0 = \rho g H/2$, B and S are the floater span and the submerged depth.

The non-dimensional time histories of dynamic motion are defined as follows:

$$x^*(t) = x(t)/(H/2), z^*(t) = z(t)/(H/2), \theta_y^*(t) = \theta_y(t)/(H/2), T_i^*(t) = T_i(t)/p_0 BS \quad (9)$$

where $x(t)$, $z(t)$, $\theta_y(t)$, $T_i(t)$ correspond to the time histories of dynamic motions in surge, heave and pitch directions, and mooring tension respectively.

3. Results and discussions

The predicted dynamic responses by the nonlinear wave theory are validated by the water tank test. The dynamic motions predicted by the linear and nonlinear wave theories are then compared in the linear, weak nonlinear and strong nonlinear regions in order to investigate the effects of nonlinear waves.

3.1. Validation

The static equilibrium test by the numerical model is performed and the initial displacements of the floater in the water tank with a depth of 1.0m are shown in the Table 2. It is can been seen that the initial displacements in six degrees of freedom are small and the model is balanced at the initial situation.

Table 2. Comparison of predicted and measured initial displacements of the floater model.

DOF	Surge(m)	Sway(m)	Heave(m)	Roll(rad.)	Pitch(rad.)	Yaw(rad.)
Experiment	0.005	-0.02	-0.0007	0.0001	0.0009	-0.003
Simulation	-0.002	0.004	0.0005	0.0006	0.002	0.001

The free decay tests in six degrees of freedom are performed for comparing the predicted natural periods of floater with the experimental data as shown in Table 3. It is clear that differences of natural periods in the surge, heave and yaw directions are very small, while the natural periods show some differences in the sway, roll and pitch directions. These differences are due to the imperfection of experiment, especially in the sway and roll directions.

Table 3. Comparison of predicted and measured natural periods of the FOWT.

Natural periods(s)	Surge	Sway	Heave	Roll	Pitch	Yaw
Experiment	5.85	18.51	2.38	3.32	3.23	5.53
Simulation	5.84	19.80	2.38	3.59	3.40	5.54

Figure 3 shows the measured and predicted RAOs of dynamic motions and tensions of mooring lines. RAOs predicted by the numerical model show good agreement with those from the water tank test . The difference between experiment and simulation in pitch for the case with a wave height of 0.02m

may be caused by the measurement errors in the water tank test because the wave height is very low in this case. It is found that the normalized surges increase linearly as the wave period increases because the wave periods are far away from the natural period of floater. A peak appears in the heave motion as a result of resonance since the wave period is close to the heave natural period of floater. It is clear that RAOs of heave motions significantly decrease with the increase of wave height. The reason is that the nonlinear hydrodynamic force is dominant in the natural period.

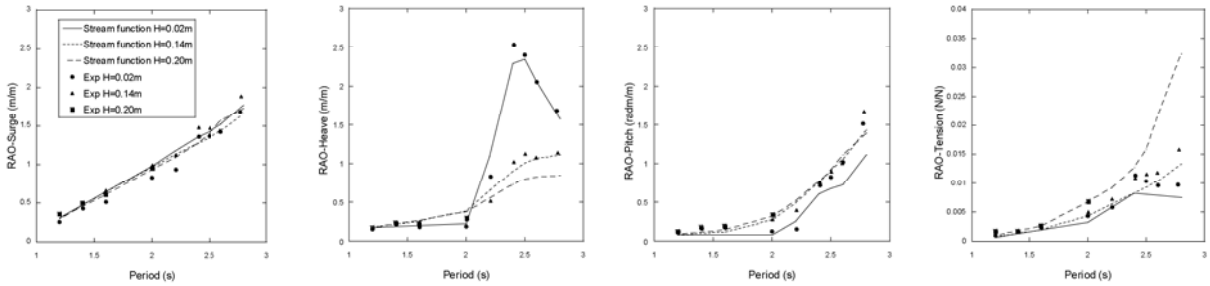

(a) Surge motion **(b)** Heave motion **(c)** Pitch motion **(d)** Mooring tension

Figure 3. Comparison of RAOs of surge, heave and pitch motions, and mooring tensions between experiments and simulations in the intermediate water.

3.2. Effects of nonlinear waves on the dynamic responses of FOWT

The comparison of RAOs of dynamic motions predicted by Airy wave theory and stream function are shown in Figure 4 for various wave heights at the wave period of 2.0s. It is clear that there are no large difference between dynamic motions by the linear and nonlinear wave theories for the waves heights from 0.02m in the linear region to 0.20m in the weak nonlinear region. In the strong nonlinear region defined near the breaking wave as shown in Figure 2, the RAOs of heave and pitch motions of the FOWT predicted by the linear wave theory are overestimated comparing with those by the nonlinear wave theory, and the overestimations become large with the increase of wave height. Furthermore, RAOs of surge motions are almost constant, while RAOs of heave and pitch motions increase with the increase of wave height at T=2.0s.

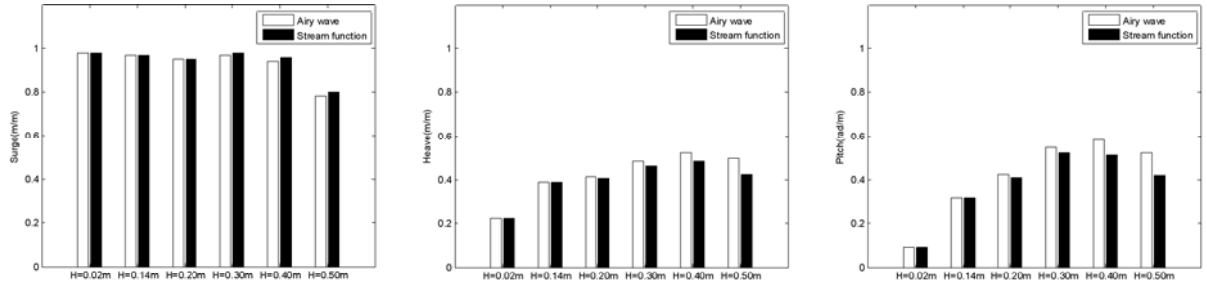

Figure 4. Comparison of RAOs of dynamic motions in surge, heave and pitch directions by Airy wave theory and stream function for different wave heights at the wave period of 2.0s.

The predicted RAOs of mooring tensions in mooring lines 1 and 3 by Airy wave theory and stream function are shown in Figure 5 for various wave heights at the wave period of 2.0s. The mooring tensions by linear wave theory are overestimated in the upstream side and underestimated in the downstream side, comparing with those by the nonlinear wave theory.

Table 4 shows the differences between RAOs of surge, heave and pitch motions and mooring tensions predicted by the linear and nonlinear wave theories. Difference between RAOs of surge by the linear and nonlinear waves is less than 4% since the surge motions are not sensitive to the nonlinear wave effects. It is obvious that there are no differences between the dynamic motions in the linear region. However, RAOs of heave and pitch motions are overestimated by 17.6% and 24.6% if the nonlinearity

of waves are not taken into account, which lead to a conservative design in the strong nonlinear region. RAOs of mooring tensions by the linear and nonlinear wave theories show no differences in the linear region, and little differences in the weak nonlinear region. In the strong nonlinear region, the linear wave theory overestimates the tension of mooring line 1 by 7.1% and underestimates that of mooring line 3 by 8.2%.

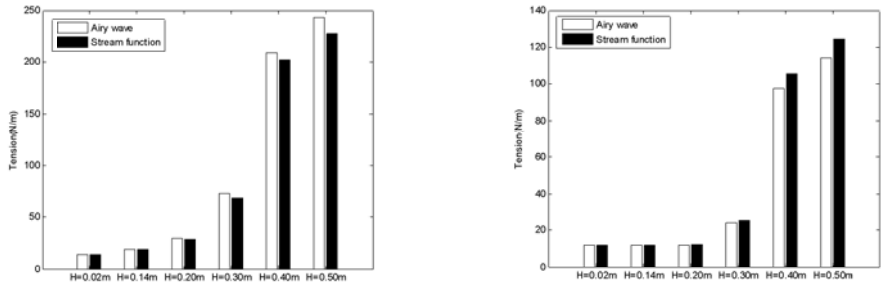

Figure 5. Comparison of RAOs of mooring tensions of line 1 (left) and line 3 (right) by airy wave and stream function for different wave heights.

Table 4. Differences of RAOs predicted by the linear and nonlinear wave theories .

Ratio	H=0.02m	H=0.14m	H=0.20m	H=0.30m	H=0.40m	H=0.50m
Surge	0	0	-1%	-1%	-2%	-4%
Heave	0	0	1.8%	4%	8%	17.6%
Pitch	0	0	3%	5%	13.6%	24.6%
Line 1	0	0.8%	3.6%	6%	3.4%	7.1%
Line 3	0	-0.7%	-2.4%	-5.2%	-7.6%	-8.2%

To explain the effects of nonlinear wave on the dynamic responses of floater, time histories and PSD of wave elevations, dynamic responses and mooring tensions in various wave heights are shown in Figure 6 and Figure 7 in the linear, weak nonlinear and strong nonlinear regions. Ten periods of data are used for the spectrum analysis. The linear and nonlinear wave theories show the same wave elevation profile and spectrum in the linear region and result in the same dynamic responses and mooring tensions. No second order motion is excited in this region because both waves and mooring lines are linear. The dynamic motions in the surge and pitch directions in the low frequency region is caused by the motions with the natural periods of floater.

In the weak nonlinear region with a wave height of 0.20m, differences of dynamic motions are less than 3% in the surge, heave and pitch directions. The nonlinearity of wave has no much effect on dynamic responses in the region, even the crest predicted by the stream function is higher than that by Airy waves and some high order components appear in the wave elevation and mooring tension. PSD of dyanmic responses shows that the pitch motion is slightly sensetive to the nonlinear wave effects, since the second order pitch motion is observed in the weak nonlinear region.

In the strong nonlinear region, the strong nonlinearity of wave is observed by comparing with wave elevations predicted by the linear and nonlinear wave theories. The nonlinear regular wave show obvious asymmety for the crest and trough and the high order components are significant. The high order components in the dynamic motions are also excited by the strong nonlinearity of mooring tensions.

The reason of overestimations of RAOs by the linear wave theory in the heave and pitch directions is that the first order component of wave elevation in the linear wave is larger than that in the linear wave. The higher order components may be important for some structures with a natural frequency in these frequency regions. The mooring tensions by Airy wave theory and the stream function have some phase differences due to the asymmetries in the wave velocity and acceleration by the stream

function.

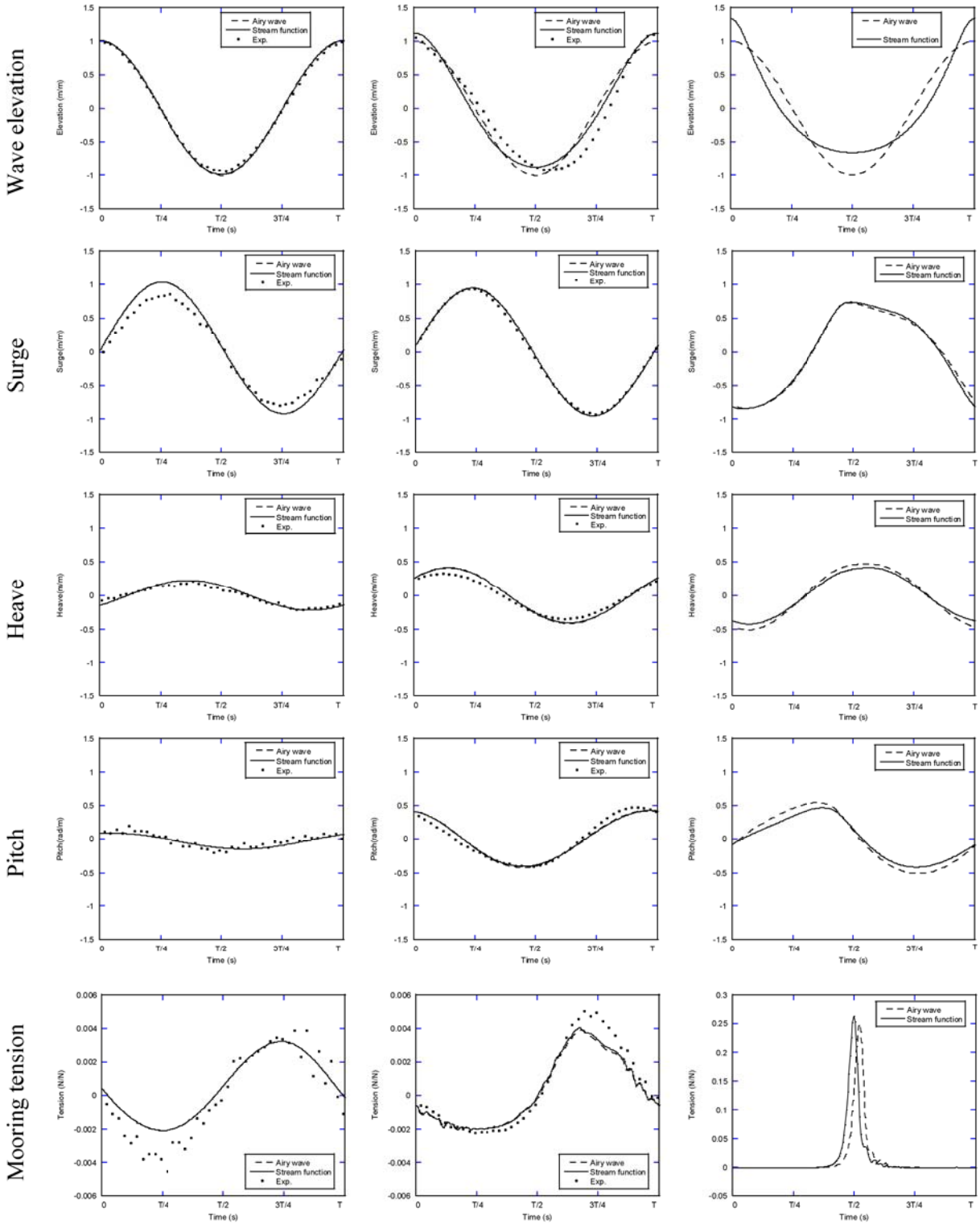

(a) H=0.02m **(b)** H=0.20m **(c)** H=0.50m

Figure 6. Comparison of time histories of normalized elevations, dynamic responses and mooring tensions, by linear and nonlinear wave theories for different wave heights.

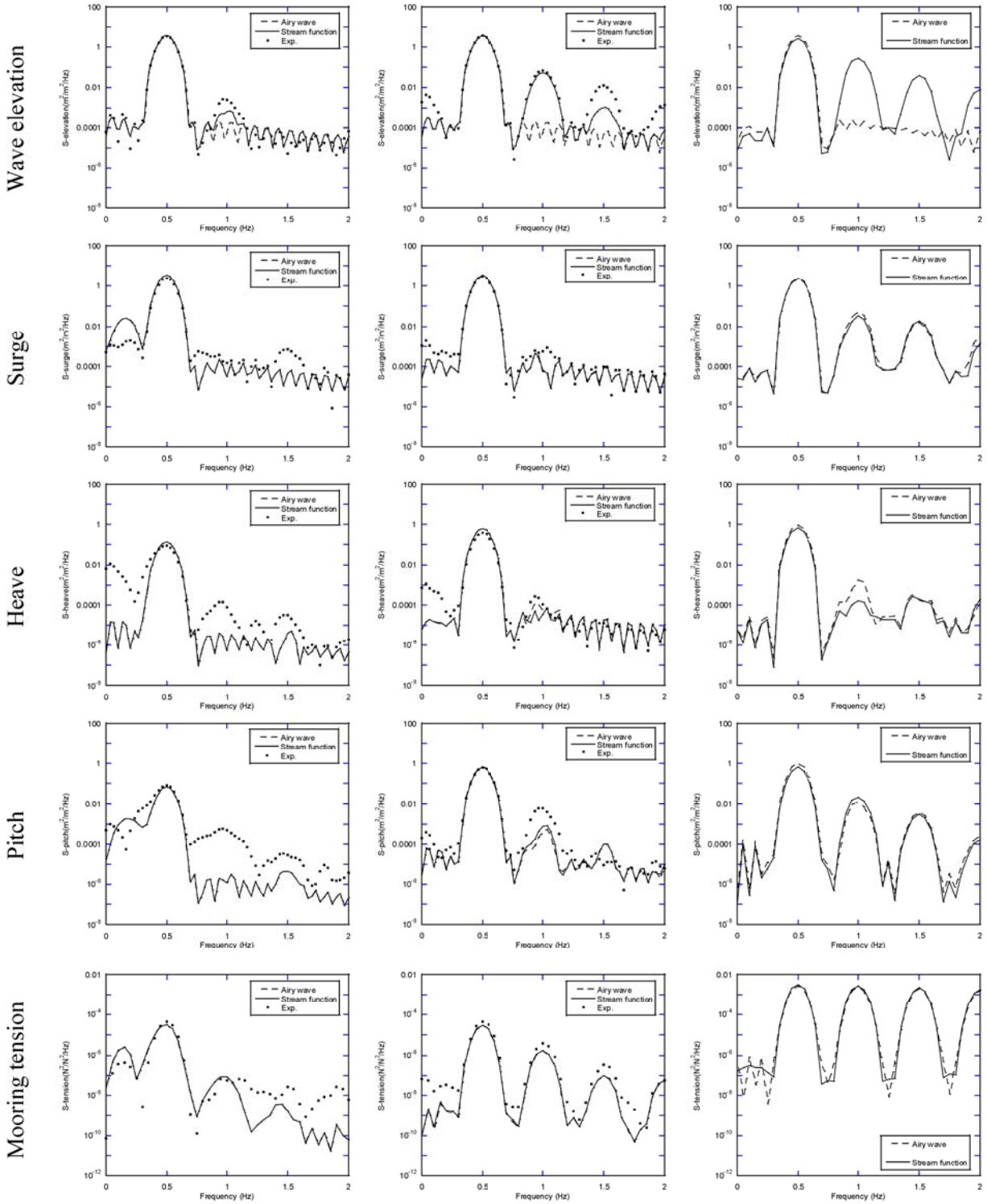

(a) H=0.02m **(b)** H=0.20m **(c)** H=0.50m

Figure 7. Comparison of PSD of normalized elevations, dynamic responses and mooring tensions, by linear and nonlinear wave theories for different wave heights.

4. Conclusions

A numerical model to predict the dynamic responses based on the potential theory and nonlinear drag force is validated by the water tank tests. Waves generated by Airy wave theory and the stream function are applied for prediction of dynamic responses of a semisubmersible floating offshore wind turbines in the intermediate water. Conclusions are obtained as follows:

1) The dynamic responses of a semisubmersible FOWT predicted by the nonlinear wave theory show good agreement with those from the water tank tests.
2) The dynamic responses and mooring tensions in the linear and weak nonlinear regions are accurately predicted by both linear and nonlinear wave theories. However, in the strong nonlinear region, the linear wave theory overestimates the heave and pitch motions by 17.6% and 24.6% and underestimates the surge motion by 4%. The mooring tensions in the upstream are underestimated, while those in the downstream are overestimated.
3) The PSDs of dynamic responses of the floater motions and mooring tensions only show the harmonic component in the linear region. The second and third order components appear in the PSDs of wave elevation, pitch motions and mooring tensions in the weak nonlinear regions, while all PSDs reveal the higher order components in the strong nonlinear wave region.

References

[1] D. Dolan, "Deepwater fixed bottom wind turbine platform", pp. 1-16, 2004.
[2] Principle Power Inc., "Principle Power's WindFloat Prototype Celebrates its 5-year Anniversary and the Final Stage of Technology Demonstration", pp. 2-3, 2016.
[3] P. Agarwal and L. Manuel, "Incorporating irregular nonlinear waves in coupled simulation and reliability studies of offshore wind turbines", *Appl. Ocean Res.*, vol. 33, no. 3, pp. 215-227, 2011.
[4] M. B. Van Der Meulen, T. Ashuri, G. J. W. Van Bussel, and D. P. Molenaar, "Influence of Nonlinear Irregular Waves on the Fatigue Loads of an Offshore Wind Turbine", *Sci. Mak. Torque from wind*, pp. 1-10, 2012.
[5] T. Ishihara, P. V, Phuc, and H. Sukegawa, "A numerical study on the dynamic response of a floating offshore wind turbine system due to resonance and nonlinear wave", In: *2nd. Europe Offshore Wind Conference*, pp. 4-6, 2007.
[6] S. K. Chakrabarti, *Hydrodynamics of offshore structures*. WIT press, 1987.
[7] IEC 61400-3, Wind turbines - Part 3: Design requirements for offshore wind turbines, 2009.
[8] R. G. Dean, "Stream function representation of nonlinear ocean waves", *J. Geophys. Res.*, Vol. 70, No. 18, pp. 4561-72, 1965.
[9] Fukushima FORWARD, http://www.fukushima-forward.jp/english/index.html
[10] S. Zhang and T. Ishihara, "Prediction of dynamic response of semi-submersible floating offshore wind turbine using Morison based theory", In: *Proc of EWEA* 2015: 17-21, 2015
[11] S. Zhang and T. Ishihara, "Numerical study of hydrodynamic coefficients of multiple hulls by large eddy simulations with volume of fluid method", In: *Offshore Wind Energy* 2017, 2017.
[12] Y. L. Liu, T. Ishihara, "Dynamic response of a semi-submersible floating wind turbine based on augmented Morison's equation", In: *Grand Renewable Energy 2018*. 2018. Yokohama.
[13] D. Ulverston, C. La, J. U. K. Telephone and W. Site, "OrcaFlex Manual", *Interface*, Vol. 44, No. 0, pp. 1-429.
[14] D. N. Veritas, "Environmental conditions and environmental loads", *DNV*, No. October, pp. 9-123, 2010.